Liquid chromatography on soft packing material, under axial compression
Size-exclusion chromatography of polypeptides

A.V. Danilov[a,b], I.V. Vagenina[a], L.G. Mustaeva[a], S.A. Moshnikov[a], E.Yu Gorbunova[a],
V.V. Cherskii[b], M.B. Baru[a,b,*]

[a]*Branch of Shemyakin and Ovchinnikov Institute of Bioorganic Chemistry, Russian Academy of Sciences, Puschino, Moscow Region*
142292, Russian Federation
[b]*SynChro Ltd., Puschino, Moscow Region 142292, Russian Federation*

Abstract

The behaviour of Sephadex G-25 gel packing for size-exclusion chromatography under dynamic axial compression in a 100×2.5 cm column of original design has been studied. The influence of dynamic axial compression on the bed structure and its chromatographic performance was determined with polypeptide samples of various molecular mass. In the studied range of compression pressure values (1.74–5.22 bar), a considerable reduction in the external bed porosity (from 0.36 to 0.20, respectively), without any collapse, is revealed. Analysis of the pressure drop on the column has shown that, under compression, the bed permeability deviates from the relationship described by the Blake–Kozeny equation. It has been found that packed bed consolidation involves not only a considerable decrease in the retention volumes but also a reduction in the distribution coefficients of substances with intermediate magnitudes of the latter ones. It can be associated with particle deformation. The influence of dynamic axial compression on the efficiency of the packed bed (zone dispersion and height equivalent to a theoretical plate), selectivity and peak resolution was studied at different eluent velocities. Compression has been shown to favour an overall increase in the resolution, with pressure optima observed in some cases. © 1997 Elsevier Science B.V.

Keywords: Axial compression columns; Packing methods; Polypeptides; Peptides

1. Introduction

The dynamic compression technique is an efficient method of high-quality column packing in preparative high-performance liquid chromatography (HPLC). A number of papers dealing with detailed studies of the phenomena in the structure of the packing obtained by this method have been pub-

*Corresponding author.

lished [1–5]. In most studies on the subject, rigid packing materials based on silicas, alumina, etc. are used. Compression of soft materials is usually supposed to cause progressive collapse, resulting in the discontinuance of normal liquid phase flow (see Ref. [5], for example).

As debates on this point are not the primary subject of this paper, it is still worth mentioning that, even without any additional external pressure, a column packing experiences compression stress of

various origins as the liquid phase flows through it. Packed beds based on soft packing materials are evidently more sensitive to such effects compared to the ones based on rigid materials, because soft materials have a lower modulus of elasticity. Practice often provides support for this point when variations in the flow-rate or viscosity of the liquid phase bring about corresponding changes in a packed bed length [6].

As regards techniques, such phenomena necessitate the use of columns with moveable pistons in order to eliminate the resultant void volume. Such bed adjustment has to be performed manually in most available column designs for the usual types of chromatography. Hence, it is impossible to eliminate the resultant void volume under the operating conditions. The use of columns with dynamic volume adaptation appears to be one of the solutions to the problem [7]. Furthermore, it would be useful to have an idea of the direction and the magnitude of variations inherent in the properties of soft packings under such an influence. Data on this point are very scarce [6,8]. Studies with the equipment realising the dynamic mode of compression could be most helpful in clarifying this issue.

It has been shown earlier for soft Sephadex G-25 [9] that its axial compression results not only in packing consolidation, as with rigid materials, but also in elastic deformation of its particles. It shows as the decrease in both the external packing porosity and the available pore volume inside the particles. The separation of Blue Dextran 2000 and potassium dichromate has demonstrated that resolution increases upon compression and the process takes less time. No dramatic reduction in the packing permeability has been observed in the studied range of pressures (from 0 to 3 bar).

The susceptibility of soft packing particles to elastic deformation upon compression and the associated changes in their inner structure can cause a variation in the packing parameters, such as retention, selectivity, etc. An investigation of the magnitude and directionality of these phenomena is the aim of this study. Size exclusion chromatography (SEC) has been chosen as a model system because it enables straightforward experimental measurement of such packing parameters as the mobile phase and stationary phase volumes and, hence, the values of

porosity and phase ratio. The last mentioned values are largely decisive for the separation efficiency, especially for SEC.

To avoid possible discrepancies, we would like to mention a number of SEC distinctions from the other chromatographic methods which motivate the peculiar terms used for describing it [10]. Since SEC is partition chromatography in essence, the stagnant liquid in the pores of the packing particles should be regarded as the stationary phase and the inter-particle liquid should be regarded as the mobile phase. V_i and V_o will further denote the volumes of the stationary and mobile phases in a column, respectively. The velocity of the mobile phase, u, is calculated in SEC according to the emergence time of an unretained component, i.e., a component that is totally excluded from the stationary phase. Thereby, u is equal to the mean velocity of the mobile phase outside the porous packing particles.

2. Experimental

2.1. Apparatus and reagents

The following chromatographic system was used in the studies: an HPLC pump type 64.00 with a preparative head (Knauer, Germany), an automatic injection system ACT-100 (Pharmacia, Sweden) with a 1250-μl loop, a column (100×2.5 cm) with a dynamic axial compression (DAC) system from SynChro (Russia), a spectrophotometer No. 87.00 (Knauer), a Shimadzu C-R6A Chromatopac integrator (Shimadzu Europe, Germany). Sephadex G-25 SF (Pharmacia) was used for column packing. The studied polypeptides from the bee venom (phospholipase A_2, EC 3.1.1.4, melittin and apamin), obtained from SynChro, contained no less than 95% of the basic substance. The synthetic analogue of oxytocin in the SH form with an additional C-terminal Lys residue was obtained by the procedure described previously [11]. Glycyl–glycine and acetic acid were of analytical grade (Reakhim, Russia).

2.2. Design of the column with dynamic axial compression

SEC of the polypeptide samples was performed on

a column of original design that was developed in our laboratory in cooperation with SynChro [12]. Fig. 1 shows the general layout of the column. The chromatographic tube is a precision bore glass cylinder (1000×25 mm I.D.). Its inner surface is carefully silanized to diminish friction. The key unit of the column is a floating piston (FP), which is steadily pressed against the gel bed via the action of the gauge gas pressure produced above it. The adapted bed length ranges from 350 to 950 mm. The FP is equipped with a special system to prevent gas penetration into the packed bed from the high pressure region. The column is equipped with a piston-position pickup for continuous monitoring of

Fig. 1. General layout of the SynChro column with dynamic axial compression.

the bed length. The minimum piston travel of 1 mm can be measured with the piston-position pickup that makes up about 0.1% of the full scale for a 100-cm column. All of the column parts in contact with working liquids are made from inert materials (glass, PTFE, titanium). The column is rated at gas or liquid pressures of up to 8 bar.

2.3. Column packing

Initially the column was packed with a 50% (v/v) suspension of the packing material in 0.2 M acetic acid, the slurry being poured into the column using an additional reservoir. A constant flow-rate of 8 ml/min was provided by the peristaltic pump attached to the column outlet. The length of the packed bed was 82.5 cm when sedimentation finished. After that, the floating piston was inserted and the system was assembled to completion.

2.4. Packing compression

At first, the packed bed was compressed to 1.74 bar and the pressure (P_{AC}) was successively increased to 5.22 bar. After each pressure rise, the column was eluted at a flow-rate of 0.4 ml/min for 12–15 h, to achieve more uniform distribution of deformation within the packed bed. The moment of termination of bed deformation was judged by the piston position pickup (the data are not reported). After that, the floating piston was fixed, to eliminate the influence of back-pressure caused by the increasing flow-rate, on the established equilibrium.

2.5. Chromatography

At each pressure value, a series of runs with separate samples was performed. The concentrations of the samples in 0.2 M acetic acid were 2 mg/ml for phospholipase A_2 (Pla), 4 mg/ml for apamin (Apa) and melittin (Mel), 2 mg/ml for the oxytocin analog (Oxy) and 10 mg/ml for glycyl–glycine (GG). A three-component mixture of Pla–Apa–GG (1.6, 1.6 and 4 mg/ml, respectively) was tested as well. The samples were eluted with 0.2 M acetic acid at a constant flow-rate (FR) of 3.2 ml/min (hereafter the data are for FR=constant). At 3.54 and 5.22 bar, two additional series of similar runs were performed
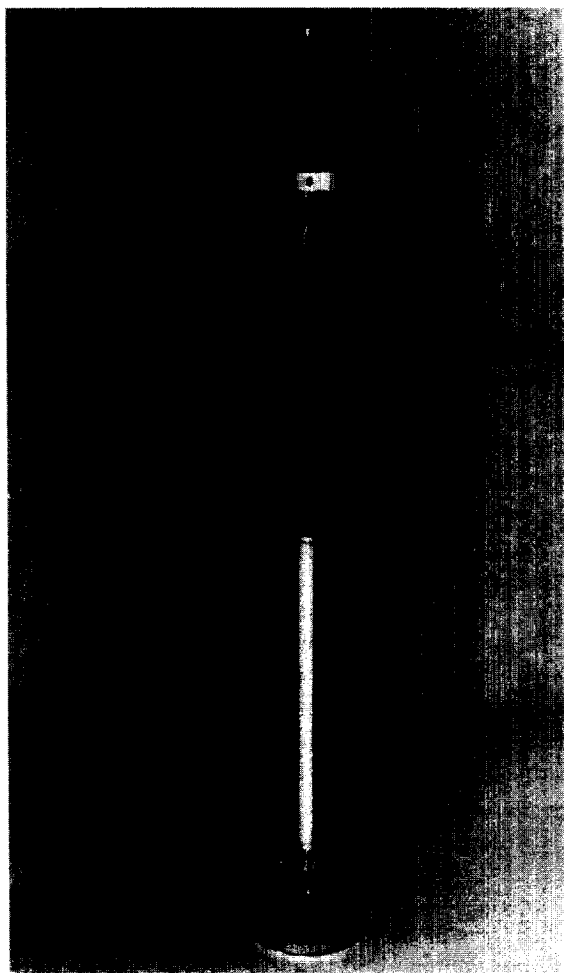
with decreasing flow-rates for each of these pressure values. The results of these additional experiments were used to interpolate the data on the retention and dispersion of the chromatographic zones, adjusted to the values of an eluent linear velocity of 1.78 cm/ min, corresponding to the value of the latter one under an initial compression pressure of 1.74 bar (hereafter the data are for u=constant). The exact flow-rate value was determined by the gravimetric method before and after each series of the experiments. The eluate adsorption was monitored at 226 nm.

2.6. Data processing

Data acquisition and initial processing was performed on the Shimadzu C-R6A Chromatopac integrator, with data being stored using a tape recorder. Dispersion of the chromatographic zones was calculated using the standard integrator function as a ratio of the peak area to its height (which is approximately equal to the peak-width at half height, $w_{1/2}$). With constant integration parameters (as was the case), this method yields somewhat underestimated peak-width values for wide peaks, and overestimated values for narrow peaks. The random error according to the data on repeated experiments does not exceed 0.5% for the retention times and volumes, or 3% for the peak widths. The $w_{1/2}$ value was also corrected for the experimentally assessed instrument contribution (non-zero injection volume, broading in the capillaries). In the calculations of peak deviation, σ, it was supposed that $w_{1/2} \approx 2.355\sigma$. When determining the errors in the calculated values, we used the method of propagation of errors.

3. Results and discussion

3.1. Structure of the packed bed

The data accounting for the changes in the structure of the packed bed with successively increasing compression pressures are shown in Fig. 2. For Sephadex G-25, the retention volume of GG (the V_t curve) and that of Pla (the V_o curve) are practically equal to the total volume of the liquid and mobile phases in the column, respectively. The V_c curve is
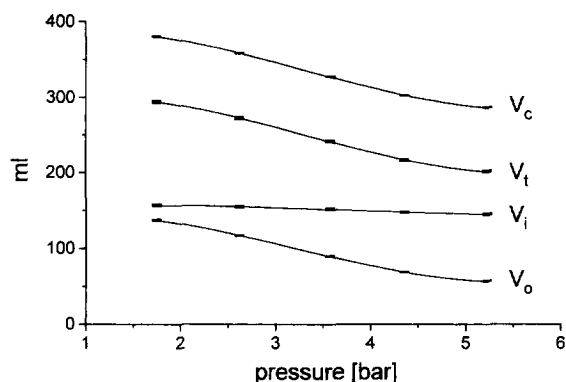

Fig. 2. Variation in the column volume (V_c), the total volume of the liquid phase (V_t), and the volumes of the mobile (V_o) and stagnant (V_i) phases for Sephadex G-25 gel by the action of DAC (see Section 2 Section 3 for conditions).

representative of the variations in the total column volume, derived as the product of the packed bed length and the cross-sectional area. The curve, denoted by V_i in the figure and derived as the difference between V_t and V_o, accounts for the change in the available volume of the stagnant mobile phase inside the packing particles. As seen from the figure, the reduction in the column's volume upon compression is caused not only by bed consolidation with the resultant decrease in V_o. As mentioned above (see Ref. [9]), compression also induces deformation of the soft particles that account for the V_i decrease, with a value that is equal to 8% of the initial V_i. As this takes place, the difference between V_c and V_t (i.e. the solid fraction of the bed) hardly changes.

Fig. 3 illustrates the resultant influence of compression on the mean external porosity, ε, derived as V_o/V_c. As the compression pressure increased from 1.74 to 5.22 bar, the ε value decreased from 0.36 to 0.20. Such a marked porosity reduction results in a corresponding increase in the column's resistance to the liquid flow. The values of the specific packing permeability, B_o, given in Table 1, were calculated by the Darcy formula [13].

$$q = -B_o \, \Delta p / \eta L \qquad (1)$$

where q is the flow-rate per unit cross-sectional area of the column, L is the bed length and η is the dynamic viscosity of the eluent. The pressure drop across the column, Δp, specified in Table 1, was
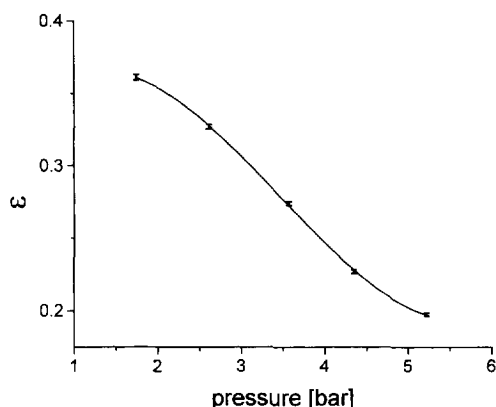
Fig. 3. Compression effect on the external porosity of the gel bed packed with Sephadex G-25. See Section 3 for conditions.

measured at a constant eluent flow-rate of 3.2 ml/min. The Blake–Kozeny equation relates B_o to the values of the external porosity, ε, and the specific surface area, a_p (m^2/m^3) of the particles [13]:

$$B_o = \varepsilon^3 / h_k a_p^2 (1 - \varepsilon)^2 \qquad (2)$$

where h_k is the empirical coefficient. Analysis of the permeability dynamics shows that for this equation to hold, the observed decrease in B_o and ε must be accompanied by a reduction in the $h_k a_p^2$ value (see Table 1). Thereby, when the compression pressure increases from 1.74 to 5.22 bar, the calculated a_p value is almost halved (see Table 1) if h_k is taken to be constant. On the other hand, as Sephadex particles are spherical initially, their a_p has its minimum value of $6/d_p$, where d_p is the particle diameter. Any variation in the shape of particles upon deformation

Table 1
Effect of DAC on the Sephadex G-25 bed porosity and related parameters

P_{AC} (bar)	ε	Δp^a (bar)	B_o [b] (μm^2)	$h_k a_p^2$ [c] (μm^{-2})	Relative a_p [d]
1.74	0.36	3	0.25±0.04	0.46±0.08	≅1
3.57	0.27	4	0.128±0.017	0.30±0.04	0.81±0.09
5.22	0.20	6	0.093±0.007	0.13±0.01	0.53±0.05

[a] Measured accurate to 0.5 bar at a constant flow-rate of 3.2 ml/min.
[b,c] Calculated by the Darcy and Blake–Kozeny equations, respectively (see Section 3).
[d] The ratio of the value $\sqrt{h_k a_p^2}$ to its magnitude at a compression pressure of 1.74 bar.

can cause only an a_p increase. Hence, our data do not fit the Blake–Kozeny equation if we assume that a_p, and consequently the particle's external surface, are independent of pressure.

This contradiction can be explained if a combination of particles inside the packed bed is considered instead of separate particles. A schematic view of the cross-section of a flow channel formed by three contacting particles is illustrated in Fig. 4 for the undeformed particles (a) and those deformed under compression (b), respectively. It may be suggested that the area of the channel walls in contact with liquid will decrease faster than the channel volume, upon compression, due to the reduction in space near the places of particle contact. Therefore, the external surface area decreases with increasing pressure. Allowing area to change with P leads to the data in Table 1.

From the physical standpoint, it is equivalent to the reduction in the specific surface area, to which the kinetic energy of the mobile phase is dissipated. It occurs mainly by elimination of narrowing sections between adjacent particles, these sections being unfavourable for the flow. Though actual changes in the bed structure are only roughly approximated by the scheme shown in Fig. 4, it enables one to explain the absence of a dramatic rise in the eluent's pressure drop when the observed external porosity decreases appreciably.

3.2. Retention

Deformation of the packed bed, accompanied by a reduction in the values of V_o and V_i, must obviously cause the corresponding changes in the retention of
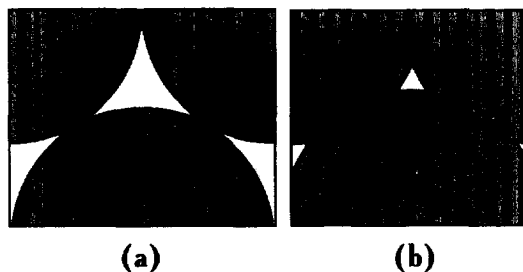

(a)   (b)

Fig. 4. Cross-section of the flow channel formed by three contacting particles: (a) undeformed particles and (b) particles deformed by the action of DAC.

substances with intermediate values of the distribution constant, K_o, as $V_R = V_o + K_o V_i$. The compression effect on the K_o value is less evident. According to the calculations (see Fig. 5), a reduction in the distribution constant is observed for all of the substances eluted in the range between V_o and V_t, with increasing compression pressure. K_o is known to depend on the interrelation between the pore diameter and the size of molecules of a fractionated substance. For example, in the simplest model with cylindrical pores and the molecules approximated by solid spheres, the distribution coefficient will be as follows ([14], p. 32):

$$K_o = (1 - \lambda)^2 \tag{3}$$

where λ is the ratio of the molecular diameter to the pore diameter. Therefore, the observed changes in the distribution constants indicate a reduction in the apparent pore size, since molecules do not change in size under these conditions. In fact, the type of mechanism responsible for the reduction in V_i is thus clarified. Narrowing of intra-particle pores upon packing contraction is most probable, and such narrowing is not necessarily uniform. Moreover, in places of particle contact, some pores probably close, i.e. particles can become inhomogeneous to some extent.

Let us consider variations in column selectivity in the process. The calibration curves, corresponding to compression pressure values of 1.74, 3.57 and 5.22 bar, are shown in Fig. 6. In addition to the shift of the curves, caused by a reduction in the retention volumes, changes in their slopes are observed, due to
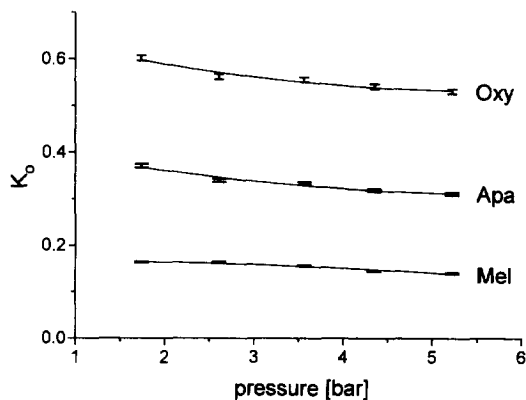

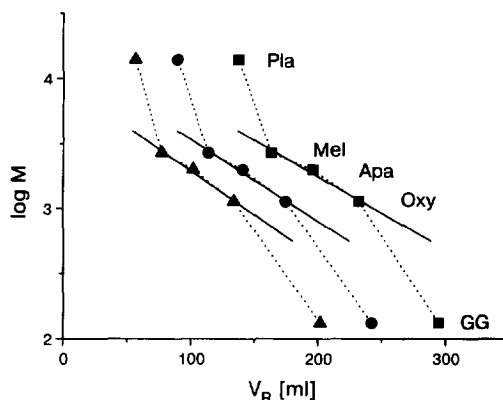Fig. 5. Distribution coefficient vs. compression pressure.

Fig. 6. Calibration curves obtained at a compression pressure of 1.74 bar (■), 3.57 bar (●) and 5.22 bar (△). The straight lines correspond to a linear regression fit of the data on Mel, Apa and Oxy.

variations in the distribution coefficients. Two portions of the presented curves with the opposite tendencies may be distinguished in this case. The slope of the curve portion with practically linear proportionality between V_R and log M increases with rising compression pressure. It means that the substances are eluted closer to each other in this range. In contrast, the portion corresponding to substances with K_o values that are close to unity becomes flatter, indicating an increase in the column's selectivity in this range.

3.3. Packing efficiency and band broadening

The classic approach to the analysis of the efficiency of chromatographic packing suggests the absence of any correlation between the purely extensive parameter of bed length and the parameter characteristic of the packing quality, i.e. the height equivalent to one theoretical plate. Besides, in most cases, the height equivalent to a theoretical plate (HETP) is supposed to depend little on retention, i.e., the former value is practically constant for all of the separated components. It means that the width of a particular chromatographic peak is proportional to the product of the square roots of the HETP and the column length:

$$\sigma = V_R \sqrt{\frac{H}{L}} \tag{4}$$

as the retention volume, V_R, is proportional to the bed length. Under the conditions of this experiment, a considerable change in both the bed length and the retention volumes is observed (see Figs. 2 and 6), while the net packing quantity remains constant. The peak widths change correspondingly. Their values, expressed in terms of $w_{1/2}$, are shown in Fig. 7 as a function of axial compression, as it determines variations of all the parameters mentioned. As seen from the figure, in most cases bed compression causes a reduction in peak widths, except for the peak of GG, which has a distinct minimum at the intermediate compression values. The differences in the dynamics of the curves, shown in Fig. 7, are evidently caused by the dissimilar effect of packing compression on the corresponding HETP and V_R values.

The dependence of HETP on retention, i.e. the K_o value, is a peculiarity of SEC among other chromatographic methods. It is due to dissimilar distribution of various substances in the system of the stationary and mobile phases (which does make the separation possible) as well as to large (up to several orders of magnitude) differences in their molecular masses and, accordingly, in their diffusion coefficients. In the SEC of polymers with low diffusion coefficients, the processes of mass transfer in the stationary and

the mobile phases mainly determine the HETP value ([14], p. 72):

$$H = H_S + H_M \tag{5}$$

where H_S stands for the stationary phase diffusion contribution and H_M for that of the mobile phase diffusion.

With no adsorption, the contribution of the stationary phase diffusion to the total plate height for porous spherical particles that are filled with the stagnant liquid phase is described with sufficient accuracy within the framework of the non-equilibrium Giddings theory [15]:

$$H_S = \frac{R(1 - R)d_p^2}{30D_S} \cdot u \tag{6}$$

where R, d_p and D_S are the relative velocity of the zone migration, the mean particle diameter and the coefficient of the intra-particle diffusion, respectively. Since $R = V_o/(V_o + K_o V_i)$, the above-mentioned equation is rearranged to give:

$$H_S = \frac{\beta K_o}{30(\beta + K_o)^2} \cdot \frac{d_p^2}{D_S} \cdot u = c_S \cdot \frac{d_p^2}{D_S} \cdot u \tag{7}$$

where $\beta = V_o/V_i$ is the phase ratio. The absolute H_S value can not be obtained because it is hard to measure the D_S value experimentally. However, possible tendencies of H_S variation can be estimated if changes in d_p are disregarded. The c_S value is a function of β and K_o, which can be determined directly from the experimental data.

c_S reaches its maximum value equal to $1/120$ at $\beta = K_o$. The values of the phase ratio and the corresponding c_S values for the studied substances as a function of the compression pressure are reported in Table 2. c_S appears to vary in different ways depending on the K_o value: it increases for small K_o (Mel, Apa) and decreases for $K_o = 1$ (GG). In the case of Oxy, β approaches its K_o upon compression and the c_S value rises correspondingly at first and begins to decrease, having gone through a maximum.

As mentioned above, pore narrowing is observed under axial compression resulting in an increase in the ratio of the molecular diameter to the pore diameter, λ. The following expression, accounting for the friction of molecules against pore walls, can
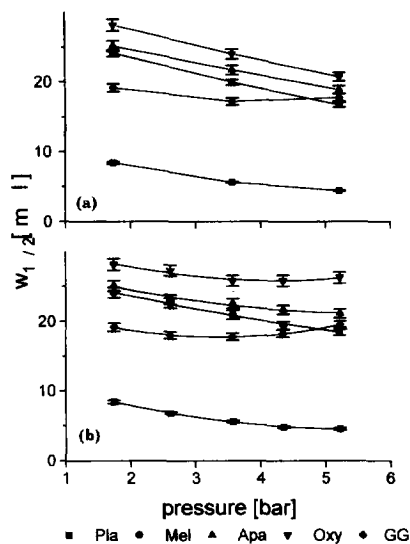

Fig. 7. Variation in peak widths caused by the action of DAC: (a) at u = constant (b) at FR = constant. See Section 2 for details.

Table 2
Effect of DAC on the parameters β, c_S, λ and relative D_S values.

P_{AC} (bar)	1.74	3.57	5.22	
β	0.88	0.59	0.39	$\pm 0.9\%$[b]
$c_S \times 30$				$\pm 1.4\%$[b]
Mel	0.133	0.166	0.194	
Apa	0.209	0.231	0.247	
Oxy	0.241	0.250	0.244	
GG	0.249	0.233	0.202	
λ				$\pm 0.5\%$[b]
Mel	0.595	0.604	0.625	
Apa	0.391	0.422	0.442	
Oxy	0.224	0.254	0.271	
Relative D_S [a]				$\pm 2\%$[b]
Mel	$\equiv 1$	0.98	0.95	
Apa	$\equiv 1$	0.95	0.92	
Oxy	$\equiv 1$	0.96	0.94	

[a] The ratio of the D_S value to its magnitude at a compression pressure of 1.74 bar.
[b] The relative error.

be used to estimate possible variations in the intra-particle diffusion coefficient [16]

$$D_S = D_M/\tau(1 - 2.104\lambda + 2.09\lambda^3 - 0.95\lambda^5) \quad (8)$$

where D_M is the diffusion coefficient in the liquid phase and τ is the factor of pore curvature (2.1–2.4). For λ estimating, it can be related to the K_o variation using Eq. (3), for example. The corresponding λ values and the relative variations in D_S are reported in Table 2. Hence, the D_S value decreases upon compression of the packing particles, which, in its turn, must cause an increase in H_S.

The second term in Eq. (5), descriptive of the eddy diffusion contribution to HETP, is determined by the formed packing structure, i.e. its homogeneity. According to the coupling theory ([17], p.54), H_M is the following:

$$H_M = \left[\frac{1}{H_f} + \frac{1}{H_D} \right]^{-1} = \left[\frac{1}{ad_p} + \frac{D_M}{c_M d_p^2 u} \right]^{-1} \quad (9)$$

where f and D subscripts denote the particular contributions to HETP of the mass-transfer processes controlled by flow and diffusion, respectively. a and c_M are parameters conditioned by the internal bed geometry. With small D_M values, the magnitude of the second term in Eq. (9) is insignificant and $H_M \approx$
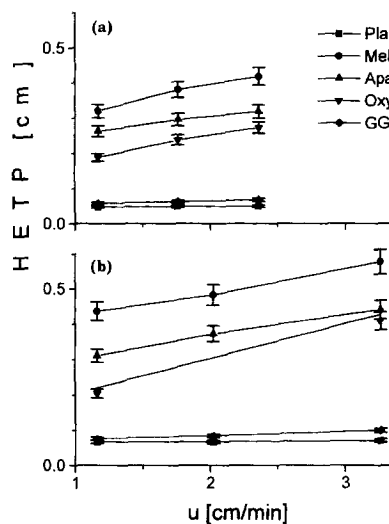

Fig. 8. HETP value vs. u: (a) at 3.57 bar and (b) at 5.22 bar.

H_f. It is also supported by the experimental results on the HETP dependence on the velocity of the mobile phase (see Fig. 8). Specifically, the HETP value remains practically constant for Pla totally excluded from the packing pores (and $H = H_M$). Following on from the coupling theory of eddy diffusion, the H_M value must be reduced for the rest of the substances, as the molecular mass decreases and the corresponding diffusion coefficient increases at the constant velocity, u.

The case of the low-molecular-mass GG is worthy of special note. With the retention time expressed in terms of the eluent linear velocity and the packed bed dimensions, there is no difficulty in obtaining the expression:

$$t_R = V_R L/V_o u = (1 + K_o V_i/V_o)L/u$$

and in the case of GG, $t_R = (1 + 1/\beta)L/u$. At $u =$ constant, the rise in compression pressure in the course of chromatography involving a reduction in the bed porosity is accompanied by a considerable increase in $1/\beta$. As this takes place, a considerable rise in the GG retention time from 92.7 min to 183.3 min is observed, in spite of diminishing L (see Fig. 10a and Fig. 10c). Thus, the enhancement of the HETP value can be brought about due to the longitudinal diffusion in the stagnant phase. In accordance with the random-walk theory ([17], p. 36), the corresponding value is:

$$H_L = b \cdot \frac{D_S}{u} \cdot \frac{1 - R}{R} = b \cdot \frac{D_S}{u} \cdot \frac{1}{b} \qquad (10)$$

where b is the obstructive factor. Hence, this HETP term must increase with decreasing phase ratio (see Table 2).

The experimental HETP values are shown in Fig. 9. $1/\varepsilon$ and $1/\beta$ have been chosen as abscissas for plotting the data obtained at the constant linear velocity and constant flow-rate, respectively, for the following reason. These values, which increase with compression, account for the integrated effect of the stress applied to the packing. Hence, the data, plotted versus $1/\varepsilon$ and $1/\beta$, are less sensitive to the inaccuracy caused by the partial friction compensation for the load applied to the packing. In addition, such HETP curves account for the process physics more adequately. Thus, the linear velocity is proportional to the $1/\varepsilon$ value at a constant flow-rate and the observed HETP increase is mostly due to its increase under these conditions. So, at a constant linear velocity of the eluent, the HETP variation is related either to the H_S value [for substances with intermediate magnitudes of K_o, see Eq. (7)], or to the H_L value [GG, see Eq. (10)], with these two values being dependent mainly on the $1/\beta$ parameter. The dampened rise in the HETP characteristic of the curves for Mel, Apa and Oxy lends support to the above considerations.
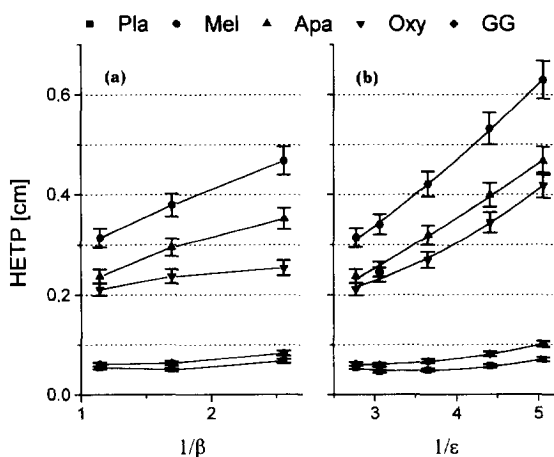

Fig. 9. HETP variation caused by the action of DAC: (a) at u =constant and (b) at FR=constant. See Section 3 for an explanation.

3.4. Resolution.

The resolution characteristics of a column may be assessed by various methods in SEC. Traditionally, the column performance has been expressed in terms of the resolution factor, R_S, for a pair of peaks

$$R_S = \frac{V_{R2} - V_{R1}}{2(\sigma_1 + \sigma_2)} \qquad (11)$$

Packing compression causes a decrease both in the retention and peak variance values. Therefore, it would be convenient to express R_S using parameters that are independent of each other. In SEC, the difference in the retention volumes of two peaks can be represented by $\Delta V_R = V_i(K_{o2} - K_{o1})$. The standard deviation of the peak can be expressed correspondingly in the same variables as $\sigma = (V_i K_o / \sqrt{N_{eff}})$ where $N_{eff} = (V_R - V_o)^2/\sigma^2$ is the effective plate number. Then, for two closely eluted peaks, the resolution factor becomes

$$R_S \approx \frac{K_{o2} - K_{o1}}{2(K_{o1} + K_{o2})} \cdot \sqrt{\overline{N_{eff}}} = \frac{1}{2} \frac{(\alpha - 1)}{(\alpha + 1)} \cdot \sqrt{\overline{N_{eff}}}$$

$$= \frac{1}{2} \cdot \varPhi \sqrt{\overline{N_{eff}}} \qquad (12)$$

where $\overline{N_{eff}}$ is the mean of the N_{eff} values of these peaks, and $\alpha = K_{o2}/K_{o1}$ is their selectivity coefficient. In the latter equation, the $\varPhi$ value accounts just for the packed bed selectivity, which is independent of the dynamic separation conditions, and the N_{eff} value is the efficiency of the bed formed. The $\varPhi$ value is constant for undeformed particles and depends on the packing material and the nature of the separated substances. As indicated above, the distribution coefficients of substances change upon compression and can result in a variation in the selectivity coefficient, α (see Table 3). As can be seen from Table 3, the $\varPhi$ value changes moderately under the present experimental conditions (increasing or decreasing within several percent) for the substances with intermediate K_o values and increases (up to 25%) for the pair of peaks with $K_{o2} = 1$.

When $K_{o1} = 0$ and the α coefficient is not defined, the resolution factor can be described by an equation similar to Eq. (12), if it is remembered that $\sigma_1 < \sigma_2$. Then

Table 3
Selectivity performance of the Sephadex G-25 bed upon DAC.

P_{AC} (bar)	α[a]			Φ[b]		
	Apa–Mel	Oxy–Apa	GG–Oxy	Apa–Mel	Oxy–Apa	GG–Oxy
1.74	2.27	1.62	1.66	0.39	0.24	0.25
3.57	2.13	1.67	1.80	0.36	0.25	0.29
5.22	2.22	1.71	1.88	0.38	0.26	0.31

[a] Selectivity coefficient, the relative error is $\approx 1.4\%$.
[b] $\Phi = (\alpha - 1)/(\alpha + 1)$ and the relative error is $\approx 2\%$.

$$R_S \approx \frac{V_i K_{o2}}{2\sigma_2} = \frac{1}{2}\sqrt{N_{eff2}} \qquad (13)$$

Table 4 indicates the N_{eff} values for different values of compression pressure at a constant flow-rate and a constant linear velocity. When the dynamics of the Φ and N_{eff} parameters are compared with the behaviour of the resolution curves (Fig. 10), it is apparent that N_{eff} exerts major control over R_S variations for the pairs of peaks with K_o close to zero. In this case, the maximum increase in resolution is observed for the pair of peaks with $K_{o1}=0$ (Pla–Mel). The increase in Φ contributes basically to the rise in the R_S value for the pairs of peaks with $K_{o2}=1$ (Oxy–GG). A maximum is typical for the curves descriptive of the resolution factor at FR = constant in the range of 3–4 bar (see Fig. 10).

SEC is traditionally used not only for separation but for the analysis of molecular mass distributions of polymers as well. In this regard, estimation of the column's performance appears to be more useful than the resolution factor for a specified pair of peaks. The linear portion of the calibration curve (see Fig. 5) obtained for similar polymers with different molecular masses can be approximated by a curve
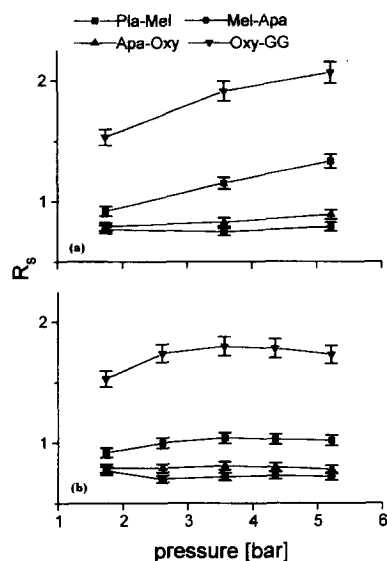

Fig. 10. DAC effect on the resolution factor for the pairs of peaks: (a) at u = constant and (b) at FR = constant.

with a slope, A, and a constant, B: $\log M = AV_R + B$ or $\Delta V_R = (\Delta \log M)/A$. Inserting the latter expression into the equation for resolution and neglecting σ variations, we obtain:

Table 4
Effect of axial compression on the effective plate number[a]

P_{AC} (bar)	at u = constant[b]			at FR = constant[c]		
	1.74	3.57	5.22	1.74	3.57	5.22
Mel	6	9	11	6	7	6
Apa	29	31	36	29	27	25
Oxy	61	67	78	61	58	46
GG	362	424	369	362	394	298

[a] The relative error in the calculated values is $\approx 6\%$.
[b] 1.78 cm/min.
[c] 3.2 ml/min.

$$R_S = \frac{\Delta V_R}{2(\sigma_1 + \sigma_2)} \approx \frac{\Delta \log M}{4\sigma A} = \frac{1}{4\sigma A} \log (M_2/M_1)$$

$$= R_{SP} \log (M_2/M_1) \qquad (14)$$

The latter expression complies with the resolution of peaks corresponding to similar polymers, their molecular masses differing by a factor of M_2/M_1. The specific resolution factor R_{SP} peculiar to SEC, equal to $1/4\sigma A$, practically does not depend on the molecular masses of the substances used for the tests. It is numerically equal to the resolution of a pair of peaks having a molecular mass difference of one order of magnitude. R_{SP} can be used for estimating and comparing the performances of different SEC columns. R_{SP} can be normalised to the bed length, thus, a certain resolution parameter corresponding to a 1-cm column is obtained:

$$R_{SP}^* = \frac{R_{sp}}{\sqrt{L}} = \frac{1}{4\sigma A \sqrt{L}} \qquad (15)$$

This criterion is helpful for comparing columns with different or varying bed lengths. The R_{SP} and R_{SP}^* values for this experiment are reported in Table 5. Interestingly, the column resolution factor R_{SP}^* increases upon compression, not only at a constant linear velocity of the eluent, but even when it rises at a constant flow-rate.

In conclusion, the elution profiles for the three-component mixture (Pla–Apa–GG) are shown in Fig. 11, to illustrate the net effect of axial compression on the SEC parameters. The (a) profile corresponds to the initial conditions, while the (b) and (c) profiles demonstrate the optimum in the separation time with good resolution and the optimum in peak resolution with a longer separation time, respectively.
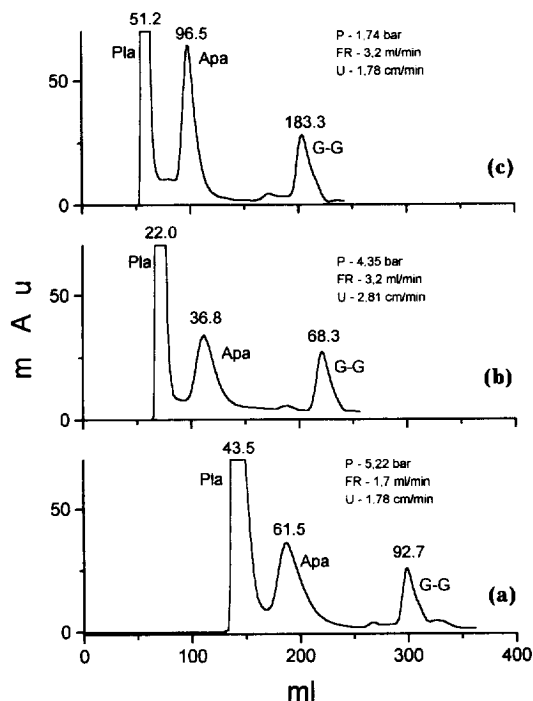

Fig. 11. Elution profiles of the three-component polypeptide mixture under the following conditions: (a) $-P_{AC} = 1.74$ bar, FR = 3.2 ml/min; (b) $-P_{AC} = 4.35$ bar, FR = 3.2 ml/min and (c) $-P_{AC} = 5.22$ bar, FR = 1.7 ml/min. The sequence of the components eluted is as follows: Pla, Apa, GG; the values above the peaks denote the retention times (min), see Section 2 for other conditions.

4. Conclusion

The experiments performed and the analysis of the obtained data have shown that the dynamic axial compression technique is applicable for packings based on soft materials. In this case the "softness" of a packing material can be estimated according to its ability to deform by the action of the pressure

Table 5
Variations in packing performance by the action of DAC.

P_{AC} (bar)	at u = constant[a]			at FR = constant[b]		
	1.74	3.57	5.22	1.74	3.57	5.22
R_{SP}	4.01±0.14	4.20±0.15	4.55±0.16	4.01±0.14	3.97±0.14	3.88±0.14
R_{SP}^*	0.46±0.016	0.51±0.018	0.60±0.021	0.46±0.016	0.49±0.017	0.51±0.017

[a] 1.78 cm/min.
[b] 3.2 ml/min.

applied. Although Sephadex G-25, which was used in this study, is considered to be rather rigid, its particles have been shown to deform in the studied range of compression pressure. The following distinctions between this packing and those based on rigid materials have been revealed in the process (see Section 3.1): (i) A considerable reduction in porosity is caused not only by bed consolidation, but by particle deformation as well; (ii) the observed deviation of the permeability–porosity relationship from the one given by the Blake–Kozeny equation seems to be responsible for the absence of a dramatic increase in the pressure drop in the column.

For SEC, a decrease in the packing porosity, phase ratio and deformation of packing particles induce qualitative and quantitative variations in the retention parameters and column efficiency. As this takes place, a reduction in dispersion of the chromatographic zones is observed for practically all of the substances studied (except GG with $K_o = 1$), due to the decrease in retention volumes in spite of the regular increase in HETP values. This, in turn, is responsible for a rise in the resolution of the column under negligible changes in selectivity.

In conclusion, one more argument can be advanced in support of the possibility of compression of soft packing materials. About 100 separations have been performed for the above experiments, and the column has been in continuous operation for about 500 h without repacking. It is essential that the packing has preserved its chromatographic properties in the process.

Acknowledgments

References

[1] H. Colin. P. Hilaireau and J. de Tournemire, LC·GC, 8 (1991) 302.
[2] D.-R. Wu and K. Lohse, J. Chromatogr. A, 658 (1994) 381.
[3] G. Carta and W.B. Stringfield, J. Chromatogr. A, 658 (1994) 407.
[4] M. Sarker and G. Guiochon, J. Chromatogr. A, 683 (1994) 293.
[5] G. Guiochon and M. Sarker, J. Chromatogr. A, 704 (1995) 247.
[6] V.H. Edwards and J.M. Helft, J. Chromatogr., 47 (1970) 490.
[7] M. Verzele, M. De Coninck, J. Vindevogel and C. Dewaele, J. Chromatogr., 450 (1988) 47.
[8] M.B. Baru and I.V. Kozlovsky-Vagenina, J. Chromatogr. A, 657 (1993) 199.
[9] A.V. Danilov, L.G. Mustaeva, I.V. Vagenina and M.B. Baru, J. Chromatogr. A, 732 (1996) 17.
[10] Recommendations on Nomenclature for Chromatography, Pure Appl. Chem., 65 (1993) 812–872.
[11] M.B. Baru, V.V. Cherskii, A.V. Danilov, S.A. Moshnikov and L.G. Mustaeva, Russian J. Bioorg. Chem., 21 (1995) 436–445.
[12] RF patent application 94018422/26. The decision on the patent grant,5 Jan 1995.
[13] R.B. Bird, W.E. Stewart and E.N. Lightfoot, Transport Phenomena, Wiley, New York, 1960.
[14] W.W. Yau, J.J. Kirkland and D.D. Bly, Modern Size-Exclusion Liquid Chromatography—Practice of Gel Permeation and Gel Filtration Chromatography, Wiley, New York, 1979, p. 32.
[15] J.C. Giddings, Anal. Chem., 8 (1966) 998.
[16] C.N. Satterfield, C.K. Colton and W.H. Pitcher, Am. Inst. Chem. Eng. J., 19 (1973) 628.
[17] J.C. Giddings, Dynamics of Chromatography, Part 1, Marcel Dekker, New York, 1965.